Published in Applied Physics B: Lasers and optics, 119, issue 1, 189-201, 2015
which should be used for any reference to this work

An experimental study of noise in mid-infrared quantum cascade lasers of different designs

Stéphane Schilt · Lionel Tombez · Camille Tardy · Alfredo Bismuto · Stéphane Blaser · Richard Maulini · Romain Terazzi · Michel Rochat · Thomas Südmeyer

Abstract We present an experimental study of noise in mid-infrared quantum cascade lasers (QCLs) of different designs. By quantifying the high degree of correlation occurring between fluctuations of the optical frequency and voltage between the QCL terminals, we show that electrical noise is a powerful and simple mean to study noise in QCLs. Based on this outcome, we investigated the electrical noise in a large set of 22 QCLs emitting in the range of 7.6–8 μm and consisting of both ridge-waveguide and buried-heterostructure (BH) lasers with different geometrical designs and operation parameters. From a statistical data processing based on an analysis of variance, we assessed that ridge-waveguide lasers have a lower noise than BH lasers. Our physical interpretation is that additional current leakages or spare injection channels occur at the interface between the active region and the lateral insulator in the BH geometry, which induces some extra noise. In addition, Schottky-type contacts occurring at the interface between the n-doped regions and the lateral insulator, i.e., iron-doped InP, are also believed to be a potential source of additional noise in some BH lasers, as observed from the slight reduction in the integrated voltage noise observed at the laser threshold in several BH-QCLs.

S. Schilt (✉) · L. Tombez · T. Südmeyer
Laboratoire Temps-Fréquence, Université de Neuchâtel,
Avenue de Bellevaux 51, CH-2000 Neuchâtel, Switzerland
e-mail: stephane.schilt@unine.ch

C. Tardy · A. Bismuto · S. Blaser · R. Maulini · R. Terazzi · M. Rochat
Alpes Lasers SA, 1-3 Passage Max-Meuron,
CH-2000 Neuchâtel, Switzerland

1 Introduction

Quantum cascade lasers (QCLs) constitute a versatile type of coherent light source in the mid-infrared spectral region. Since their first demonstration in 1994 [1], they have been widely used in numerous applications, primar-ily in the fields of molecular spectroscopy and trace gas sensing, but also in free-space mid-infrared optical com-munications and in infrared countermeasure systems for civil and military aircrafts. Novel applications of QCLs in very high-resolution spectroscopy and optical metrology have emerged in the last years, in particular in combination with optical frequency combs [2–5], which are generally more demanding in terms of low frequency-noise and nar-row spectral linewidth. QCLs have the potential to achieve very narrow linewidths with an intrinsic value of a few hundreds hertz only [6, 7] resulting from their close-to-zero Henry's linewidth enhancement factor [8]. However, a narrow linewidth is generally not achieved in practice in free-running QCLs as a result of the presence of undesired noise that compromises their spectral properties. Hence, the char-acterization and understanding of the origin of frequency noise spectrum of free-running QCLs gained a significant interest in the recent years. A few research groups reported experimental frequency noise spectra for QCLs produced by different manufacturers and operated at temperatures ranging from cryogenic [7, 9] up to room temperature [6, 10, 11]. Significantly different levels of noise have been observed in the considered QCLs, leading to linewidths in the range of sub-100 kHz [6] to many megahertz [7]. However, no convincing justification has been given at that time to explain the large noise variability observed between these different devices. Also the large noise varia-tion that we observed as a function of temperature in some devices [12] was not fully understood. Therefore, a better

understanding of the origin of noise in QCLs appears as an important step for a possible design and realization of low-noise mid-infrared lasers in the future. Very recently, a detailed theoretical model of noise in QCLs was pro-posed by Yamanishi et al. [13] based on fluctuating charge-dipoles, which convincingly explained the flicker (1/*f*) noise observed in their ridge-waveguide QCLs.

An important outcome from some former experimental studies was the assumption [14] and subsequent experimental demonstration [12, 15] that frequency noise results from some internal electrical fluctuations arising within the QCL structure. As a result of this significant electrical flicker noise, the use of an external cavity configuration did not lead to a narrower short-term linewidth [16] than typically encountered in DFB-QCLs. Therefore, the only way to achieve narrow-linewidth QCLs so far has been based on the use of some active noise reduction techniques, such as by frequency stabilization to an optical frequency reference (e.g., a molecular transition [17, 18] or the reso-nance of a Fabry–Perot cavity using electronic [19] or opti-cal feedback [20]). As an alternative, other active methods have recently been proposed to reduce frequency noise in QCLs by exploiting the correlation arising between fluctua-tions of the optical frequency and of the voltage between the QCL terminals [15, 21] that will be further discussed in the present work. A reduction in the frequency noise power spectral density (PSD) by one order of magnitude was thus achieved by stabilizing the internal temperature of the active region in a 4.5-μm QCL using optical control with a near-infrared laser source [15]. More recently, a similar noise reduction was achieved with an all-electrical method to control the electrical power dissipated in a QCL emitting at 7.9 μm [21].

In this paper, we present an experimental study of noise in QCLs of different designs with the objective to better understand its origin. This is a first step toward the possibility to design QCLs for low-noise and narrow-linewidth operation in the future. So far, some isolated devices have shown low-noise operation, but for uncontrolled and unknown reasons (see for instance the laser used in Ref. [6]). The approach reported here to investigate noise in QCLs was based on the combination of an experimental study realized over a large set of QCLs with some modeling and statistical data analysis. By directly involving the QCL manufacturer Alpes Lasers, this study gave access to a large number of devices, in which the noise has been measured in different operating conditions (QCL temperature and current). By selecting very different types of devices made of different structures (e.g., ridge waveguide versus buried heterostructure), with different geometrical parameters (width, length, etc.) and fabricated in different processes, this study aimed at experimentally identifying some parameters that have the most prominent influence on the QCL noise. This was assessed by a statistical method based on an analysis of variance (ANOVA) of the measured noise.

This article is structured as follows. Section 2 describes the framework of this study, including the experimental setup and the selection of the lasers that have been studied. Section 3 presents some experimental results about the correlation observed between voltage noise and frequency noise in QCLs and demonstrates that the major contribution to the frequency noise originates from some electrical noise induced in the QCL structure by the electrons flow. The conversion mechanism of this electrical noise into optical frequency noise is discussed as well. Then, Sect. 4 reports the main results of the experimental noise study and pre-sents the associated statistical analysis. Finally, discussion and the conclusion of this work are presented in Sect. 5.

2 Framework of the QCLs noise study

2.1 Selection of relevant parameters and devices for the experimental study

The objective of this experimental study was to identify parameters that play a central role in the generation of flicker frequency noise in QCLs. Electrical flicker noise has been studied for a long time in various semiconduc-tor structures in general and has been interpreted by two debated models based on carrier number fluctuations [22] and mobility fluctuations [23]. However, no confident conclusion on the correctness of these models has yet been assessed, and the microscopic origin of flicker noise in semiconductors has remained misunderstood, especially in the case of more complicated structures like QCLs that are composed hundreds of layers of different composition. The very recent work of Yamanishi et al. [13] proposed a theoretical interpretation of flicker noise in QCLs in terms of the so-called fluctuating charge-dipoles model. In this model, fluctuating charge-dipoles induced by electrons trappings and de-trappings in the QCLs injector superlattices are considered to generate the flicker noise. In parallel to Yamanishi's theoretical analysis, we chose a different approach to investigate flicker noise in QCLs, based on experimental observations and a statistical analysis. An approach commonly used in process optimization was followed to identify cause-and-effect relationships between device configurations and noise variability. By perform-ing noise measurements in a variety of different QCLs, we aimed at obtaining experimental evidence on the noise vari-ability between the devices, but it was out of the scope of this work to present a microscopic model of the noise as addressed in Ref. [13]. For this purpose, some parameters were initially defined as being potentially a prominent noise

contributor in QCLs. By excluding parameters that were estimated to be less influent or that could not be experimentally tested, a set of five major independent parameters was selected, which encompassed (1) the type of process (ridge waveguide—RWG—or buried heterostructure—BH), (2) the length of the laser chip, (3) the width of the active region, (4) the operating current, and (5) the laser heat sink temperature. As the significance of each parameter on the noise variability was unknown a priori, the largest spread between possible modalities of the selected parameters was preferred, with the additional constraint to achieve laser threshold for all devices within a given temperature window.

The realized study necessitated a variety of lasers with different parameters operating within an adequate spectral region, including devices that were not necessarily optimum, in order to lead to an observable noise variability. A device selection strategy was thus adopted based on identifying existing QCLs available at Alpes Lasers at various production stages, ranging from un-singulated chips on a wafer to mounted devices. Among the huge number of potential lasers, 22 devices have been selected and tested. These lasers were issued form six different processes, four layers, and three individual growers as listed in Table 1. They are composed of two types of laser geometries as schematized in Fig. 1, and each device is composed of 35 cascaded periods. The first configuration is the ridge laser where the waveguide is surrounded by a Si_3N_4 layer acting as an optical confinement medium. The second configuration is the buried heterostructure where the active region is buried into an isolating material acting as an optical confinement medium.

Whereas the ridge-waveguide lasers are based on a bound-to-continuum design [24] and were grown by molecular beam epitaxy (MBE), all the other devices are of the 2-phonon type [24] and were grown by metal-organic vapor phase epitaxy (MOVPE). A detailed list of QCLs studied in this work is given in Table 2 together with their main parameters. All devices were operating in a similar voltage range of 7–10 V.

Table 1 List of the different processes used in the selected QCLs

Process	Layer	Grower	Geometry	Growth type	Design
1	A	1	BH	MOVPE	2ph
2	B	2	BH	MOVPE	2ph
3	C	3	RWG	MBE	b2c
4	B	2	BH	MOVPE	2ph
5	D	1	BH	MOVPE	2ph
6	D	1	BH	MOVPE	2ph

BH buried heterostructure, *RWG* ridge waveguide, *2ph* 2-phonon, *b2c* bound-to-continuum

2.2 Experimental setup

We investigated noise in QCLs using the experimen-tal setup depicted in Fig. 2. The QCLs were mounted in a standard laboratory laser housing package from Alpes Lasers and were driven by a home-made low-noise controller. The controller incorporates a highly stable thermal regulator that stabilizes the QCL temperature to better than 1 mK, and a low-noise current source capable of delivering up to 600 mA at 20 V compliance voltage or 1 A at 14 V. The current source has a noise spectral density lower than 1 nA/Hz$^{1/2}$ at Fourier frequencies higher than 1 kHz and a slightly increasing noise at lower frequency when measured on a pure resistor at similar operating voltage and current as typically used in the QCLs. With the typical cur-rent-tuning coefficient of the QCLs considered in this study (0.2–1 GHz/mA), this noise level enabled us to observe the frequency noise induced in the laser itself, without techni-cal limitation resulting from the current driver [25]. The use of such a low-noise current source was thus a prereq-uisite for the experimental investigation of noise generated within the different laser structures.

The QCLs frequency noise was measured using a spectroscopic setup as implemented in former studies [7, 10–12]. The side of a molecular transition was used as a frequency-to-intensity converter (a so-called frequency

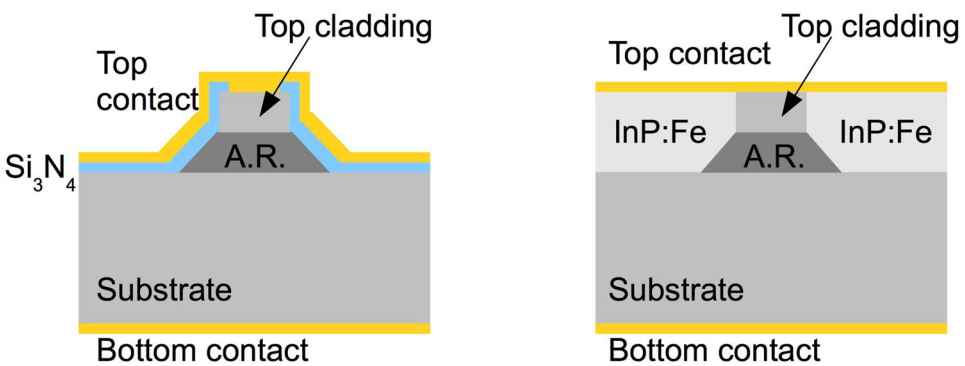

Fig. 1 Schematic representation of the ridge-waveguide (*left*) and BH (*right*) geometries used in this study. *AR* active region

Table 2 List of the lasers investigated in this study with their respective parameters

Nos	Laser	Process	Type	Length (mm)	Width (μm)	I_{roll} (mA)	J_{max} (kA/cm^2)
1	sbcw3919	1	BH	1.5	12.5	480	2.56
2	sbcw3755	1	BH	1.5	12.5	510	2.72
3	sbcw3910	1	BH	1.5	9.5	420	2.95
4	sbcw3917	1	BH	1.5	9.5	380	2.67
5	sbcw3920	1	BH	1.5	6.5	230	2.36
6	sbcw3655	1	BH	2.25	12.5	740	2.63
7	sbcw4313	1	BH	2.25	7.5	500	2.96
8	sbcw3913	1	BH	3	7.5	450	2.00
9	sbcw4818	2	BH	2.25	13	980	3.35
10	sbcw4822	2	BH	2.25	13.3	1,000	3.34
11	sbcw4817	2	BH	2.25	8.3	650	3.48
12	sbcw4821	2	BH	2.25	8.3	730	3.91
13	sbcw1035	3	RWG	1.5	~14	550	2.62
14	sbcw1037	3	RWG	1.5	~14	630	3.00
15	sbcw1028	3	RWG	1.5	~10	370	2.47
16	sbcw1027	3	RWG	1.5	~9	330	2.44
17	sbcw1045	3	RWG	1.5	~9	340	2.52
18	sbcw5501	4	BH	1.5	9.5	370	2.60
19	sbcw5502	4	BH	2.25	8	420	2.33
20	sbcw5503	4	BH	2.25	12	520	1.93
21	sbcw2921	5	BH	1.5	10	420	2.80
22	sbcw3329	6	BH	3	10	630	2.10

J_{max} represents the maximum current density. The set of devices consists of 5 ridge-waveguide (RWG) lasers and 17 BH lasers

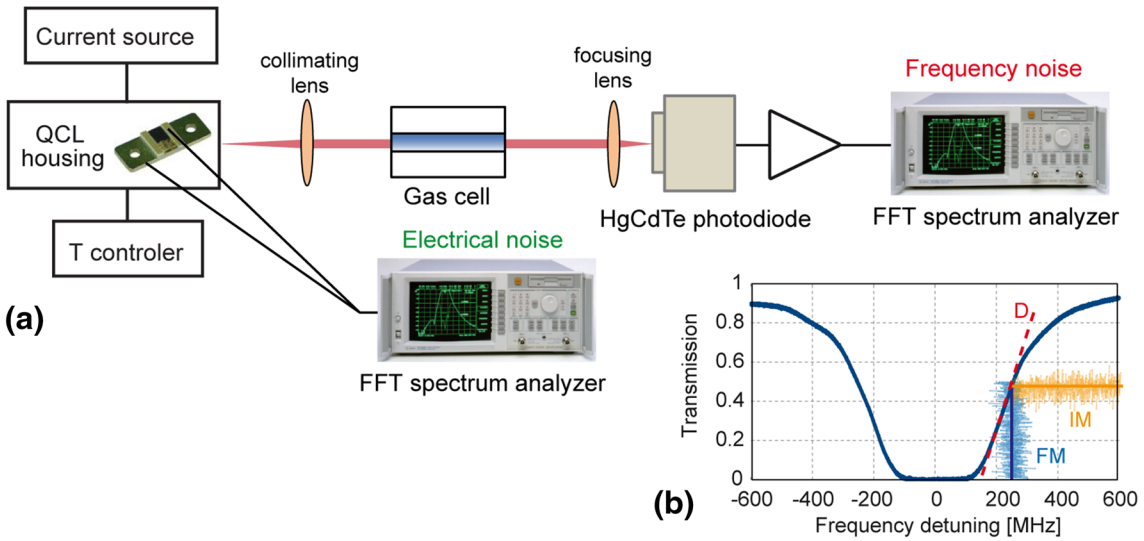

Fig. 2 **a** Schematic of the experimental setup used to measure both frequency noise and electrical noise in QCLs. **b** Principle of the use of a molecular transition to convert fluctuations of the laser frequency (FM) into intensity fluctuations (IM) that are detected by a photodiode

discriminator). Here, a 10-cm-long sealed glass cell filled with 2 mbar of pure N_2O was used with QCLs emitting in the 7.6–8 μm wavelength range. A similar cell filled with pure CO was also used with some QCLs emitting at 4.5 μm that were considered as well for some measurements in this work. In any case, the laser was tuned to the side of a suitable molecular absorption line where frequency fluctuations were effectively converted into intensity fluctuations that were subsequently detected with a photodiode as schematized in Fig. 2a. The PSD of the resulting photodiode voltage noise was measured using a fast Fourier transform (FFT) spectrum analyzer. The recorded data were

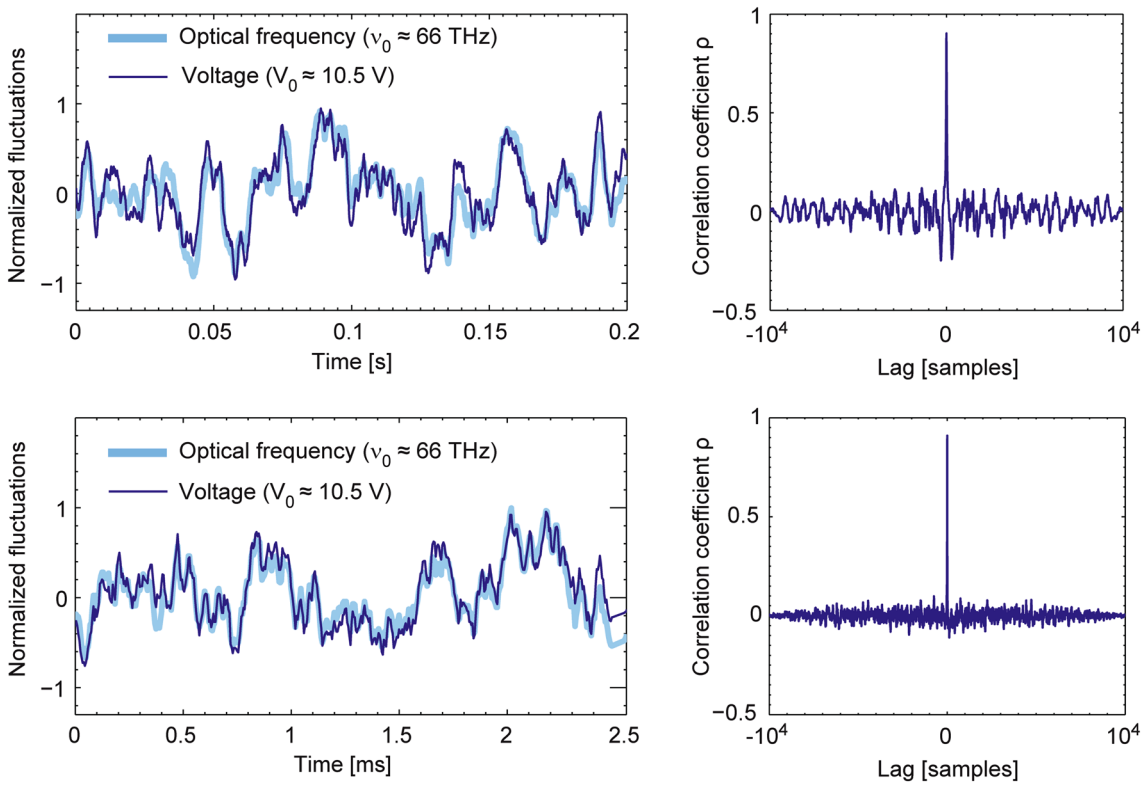

Fig. 3 *Left* Time evolution of the normalized optical frequency (*thick light lines*) and voltage (*thin dark lines*) fluctuations simultaneously measured in a 1–kHz bandwidth. *Right* Correlation coefficient between QCL voltage and optical frequency as a function of the lag between the two time series. Results are shown here for two types of QCLs operating at 4.5 μm: a ridge-waveguide laser (*top*) and a BH laser (*bottom*)

then converted into frequency noise PSD using the measured slope *D* on the side of the absorption profile shown in Fig. 2b.

In addition to frequency noise, the noise on the volt-age between the QCLs terminals was also recorded as we previously observed a high correlation between fluctuations of the QCL voltage and optical frequency [15, 21]. In Sect. 3.1, we will present some more quantitative results about the correlation between these two types of noise. Based on these results, the voltage noise across the QCL terminals appears as a simple and powerful tool to investigate noise in QCLs. Therefore, the noise study was performed essentially by investigating the QCL voltage noise. Noise spectra were usually measured at two different QCL temperatures of 25 and 5 °C. At each temperature, noise spectra were recorded at a variety of about 15 different cur-rents ranging from sub-threshold to rollover. Therefore, a massive set of noise spectra was recorded, containing more than 600 spectra.

All noise PSDs were recorded using an FFT spectrum analyzer (model Stanford Research SR-760 or SR-770) in the range of 0.1 Hz–100 kHz. In order to obtain clean measurements with a good spectral resolution over the entire considered frequency range, each spectrum was obtained from the combination of several FFT spectra measured in different frequency ranges (one spectrum for each frequency decade), after co-averaging 5,000 individual FFT traces.

3 Electrical and optical noise in QCLs

3.1 Noise correlation

Following the high qualitative correlation that we previously observed between the fluctuations of the QCL voltage and optical frequency [15, 21], we present here additional quantitative results of this effect obtained in QCLs operating at 4.5 μm. These results motivated the noise analysis presented later in this article, which was mainly based on the investigation of electrical noise in QCLs. Correlation measurements were performed in both the time and spectral domains for two types of QCLs, a BH and a ridge laser. Figure 3 (left) shows the normalized time series of voltage and optical frequency fluctuations simultaneously measured in a 1 kHz bandwidth for each laser, showing

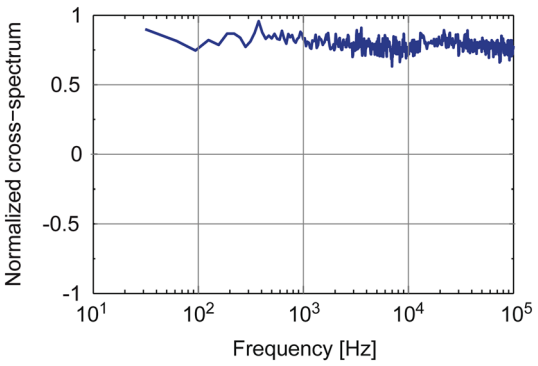

Fig. 4 Coherency spectrum between the fluctuations of the voltage and optical frequency measured in a 4.5 μm QCL showing a constant value of ≈0.8 up to 100 kHz Fourier frequency, which was the upper limit of the spectrum analyzer used in the measurement

highly correlated traces in both cases. From these data sets, the linear correlation coefficient $\rho_{\nu V}$ between fluctuations of the optical frequency ν and of the QCL voltage V was computed from the covariance $\sigma_{\nu V}$ of the time series normalized by the product of the variance of each variable, σ_ν and σ_V:

.

$$\rho_{\nu V} = \frac{\sigma_{\nu V}}{\sigma_\nu \sigma_V} = \frac{\sum_{i=1}^{n} (\nu_i - \bar{\nu})\left(V_i - \bar{V}\right)}{\sqrt{\sum_{i=1}^{n} (\nu_i - \bar{\nu})^2} \cdot \sqrt{\sum_{i=1}^{n} \left(V_i - \bar{V}\right)^2}}. \quad (1)$$

Figure 3 (right) displays the computed correlation coefficient as a function of the time lag between the two time series. A high degree of correlation of $\rho_{\nu V} \cong 0.9$ is obtained for each laser at zero time lag.

In addition, the correlation between voltage and optical frequency was also quantified in the spectral domain for one of these lasers. This was achieved by computing the normalized cross-spectrum [26] $\gamma(f)$, or coherency spectrum, given by:

$$\gamma(f) = \frac{S_{\nu V}(f)}{\sqrt{S_\nu(f) \cdot S_V(f)}}, \quad (2)$$

where $S_{\nu V}$ is the cross power spectrum of the two variables $V(t)$ and $\nu(t)$, while S_V and S_ν are the individual power spectra. The cross-spectrum $S_{\nu V}$ could not be directly measured in our experiments and was instead obtained from the measured spectra of the sum and difference of the optical frequency and voltage signals after proper amplification. Indeed, the cross-spectrum of two independent variables x and y can be written as $S_{xy} = (S_{x+y} - S_{x-y})/4$. The resulting coherency spectrum is displayed in Fig. 4. The achieved constant degree of coherence $\gamma \approx 0.8$ obtained in the entire frequency range of this measurement is similar to the single value previously assessed from the time-domain measurements.

3.2 Voltage-to-frequency noise conversion

The conversion mechanism between electrical (voltage) noise and optical frequency noise is mainly thermal: The voltage fluctuations δV measured across a QCL driven at a constant current I_0 induce fluctuations $\delta P = I_0 \cdot \delta V$ of the electrical power dissipated in the QCL structure. The thermal resistance R_{th} of the laser represents the temperature increase δT produced by a change δP of the dissipated electrical power: $\delta T = R_{th} \cdot \delta P$. The temperature variation in turn induces a fluctuation of the optical frequency $\delta\nu = (\Delta\nu/\Delta T) \cdot \delta T$, where $\Delta\nu/\Delta T$ is the laser temperature-tuning coefficient. The thermal resistance can be experimentally determined from the power- and temperature-tuning coefficients of the laser [27], $R_{th} = (\Delta\nu/\Delta P) \cdot (\Delta\nu/\Delta T)^{-1}$, or alternately by introducing the current-tuning coefficient: $R_{th} = (\Delta\nu/(V_0 \Delta I)) \cdot (\Delta\nu/\Delta T)^{-1}$. By combining the aforementioned expressions, the fluctuations of the laser optical frequency are directly linked to the fluctuations of the voltage between the QCL terminals:

$$\delta\nu = \frac{\Delta\nu}{\Delta T} R_{th} I_0 \delta V = \frac{I_0}{V_0} \frac{\Delta\nu}{\Delta I} \delta V. \quad (3)$$

From this expression, the frequency noise PSD S_ν can be assessed with a good precision from the noise spectrum of the QCL voltage S_V if the other laser parameters are known, such as the operating conditions (I_0, U_0) and the tuning coefficients $\Delta\nu/\Delta I$ and $\Delta\nu/\Delta T$. The measurement of the voltage noise is much simpler and more straightforward than the frequency noise, as it does not require any frequency discriminator and can even be realized in a larger range of experimental conditions where optical measurements are not possible, for instance below the laser threshold or for lasers that do not emit within a suitable molecular transition. This makes the study of the voltage noise, a powerful tool to investigate noise in QCLs, which was the main approach of our work. The validity of the conversion between voltage noise and frequency noise is illustrated for one laser of our study (#sbcw-3920) in Fig. 5, which compares the frequency noise measured optically using a N_2O absorption line with the equivalent frequency noise assessed from Eq. (3) using the voltage noise and other laser parameters that were independently measured. An excellent agreement is observed between the two curves, which confirms that electrical noise generated in the QCL structure also constitutes the main contribution to the frequency noise in QCLs emitting in the 7–8 μm range, as previously demonstrated with shorter-wavelength QCLs [12, 28]. This justifies our choice to mainly investigate the electrical noise of QCLs in this study.

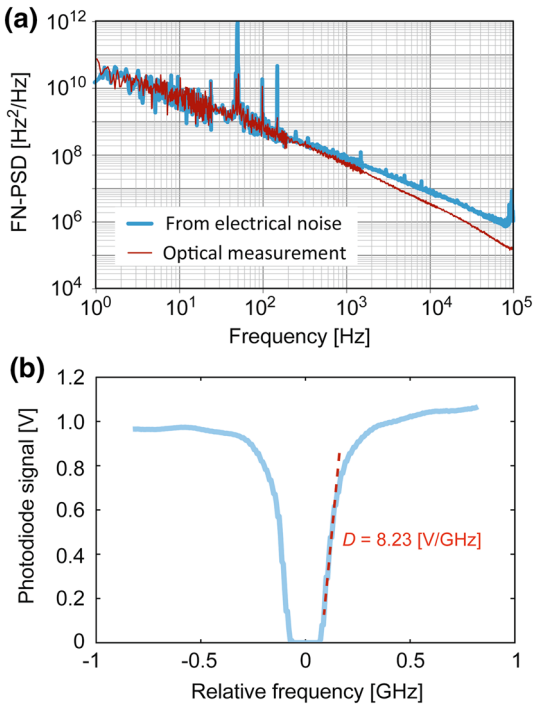

Fig. 5 **a** Comparison of the frequency noise (FN) PSD measured optically (*thin red line*) and assessed from the voltage noise across the laser (*thick blue line*) for QCL #sbcw-3920. The slight difference observed at high frequency results from the laser thermal dynamics [29]. **b** View of the N_2O absorption line used for the measurement, together with the determined discriminator slope D (*dashed line*)

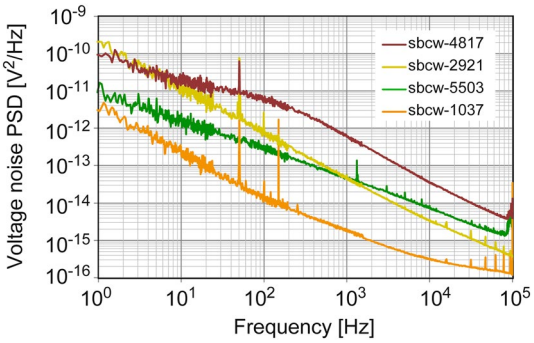

Fig. 6 Some representative voltage noise spectra measured at $T = 25$ °C in four different QCLs emitting in the range of 7.6–8 μm. Laser #sbcw-1037 is a ridge-waveguide laser, and all the others are BH lasers

4 Main results of the noise study

4.1 Raw noise spectra

A few representative voltage noise spectra measured in this study for different QCLs are displayed in Fig. 6, which shows a large noise variability spanning over more than two orders of magnitude between lasers with differ-ent structures or produced in different processes. One also notices significantly different slopes in the flicker noise of these lasers, and even the presence of two different slopes in some spectra (e.g., in laser #sbcw-4817 shown in Fig. 6). This tends to indicate that different mechanisms may con-tribute to the noise generation in these lasers.

Generally, lasers from the same process showed a similar level of noise as illustrated in Fig. 7 for two different types of process. In particular, all lasers from series sbcw-48xx showed a similar change in the slope of their flicker voltage noise from $\alpha \approx -1$ at high frequency to $\alpha \approx -2/3$ at lower frequency. The reason for this behavior is not yet understood, but it seems that a particular effect occurs in these lasers that are all produced from the same process. This effect has been observed at the two considered temperatures of 25 and 5 °C, and the exact same behavior was also obtained when driving these lasers with a commercial QCL driver for cross-check, which excludes a measurement artifact due to our home-made QCL controller.

Additional optical measurements of frequency noise and intensity noise were performed with one laser of this series (model #sbcw-4821) for further check and comparison with the measured electrical noise. Frequency noise was measured at a single QCL temperature and current ($T = 6$ °C, $I = 590$ mA) coinciding with the side of a N_2O transition, whereas intensity noise was measured out of any N_2O absorption line at a given QCL temperature ($T = 10$ °C) and at various currents ranging from thresh-old to rollover ($I = 560$–730 mA). All these spectra are displayed in Fig. 8 and show the same characteristic transition from $\sim f^{-1}$ noise at high frequency to $\sim f^{-2/3}$ noise at low frequency. The transition frequency between these two regimes increased from a few tens of hertz up to a kilohertz when the QCL drive current was increased in all the lasers of this series. Unexpectedly, one also observed a different noise dependence as a function of the drive current at low and high frequencies: The noise increases with increasing current at high frequency, but decreases at low frequency.

A summary of the voltage noise dependence measured as a function of the operation current in all the investigated lasers is displayed in Fig. 9. Here, the noise at a Fourier frequency component of 3 kHz was considered for the comparison of the different lasers, as used in former studies [12]. A large noise variability is observed among the lasers. In particular, one notices that ridge-waveguide lasers clearly show a lower noise than BH lasers as was previously observed in QCLs at 4.6 μm [28]. Very different noise dependences as a function of the drive current are also observed among the lasers: In some devices, the noise increases significantly with the current (e.g., in devices #sbcw-3920, #sbcw-3921 or #sbcw-3329), while the dependence is much weaker in some other devices (e.g., in

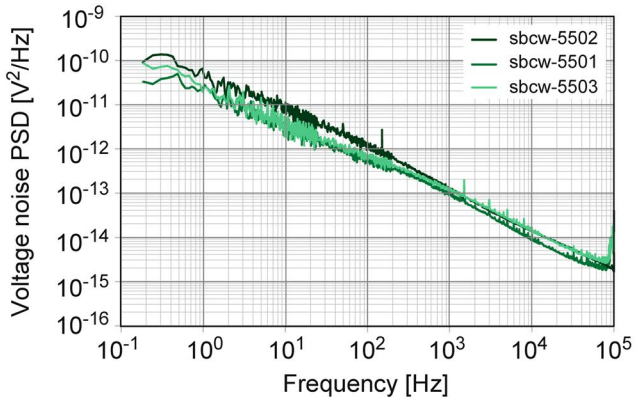

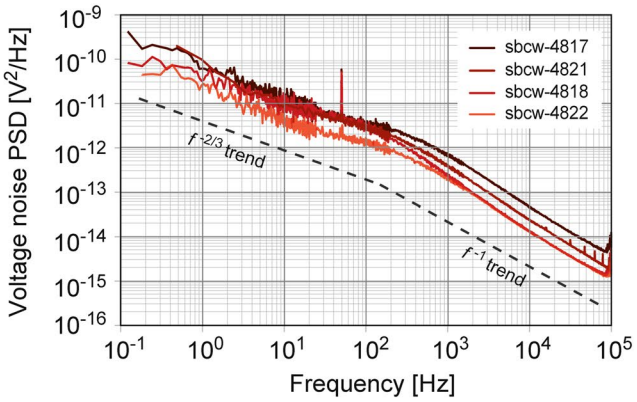

Fig. 7 Comparison of the voltage noise measured in different lasers produced from the same process showing similar noise level and behavior. *Left* Three lasers of series sbcw-55xx measured at $T = 25$ °C and $I = 360$ mA. *Right* Four lasers of series sbcw-48xx measured at $T = 25$ °C and $I = 500$ mA. The *dashed lines* are a guide for the eye displaying a slope $\alpha = -1$ and $\alpha = -2/3$ at high and low frequency, respectively

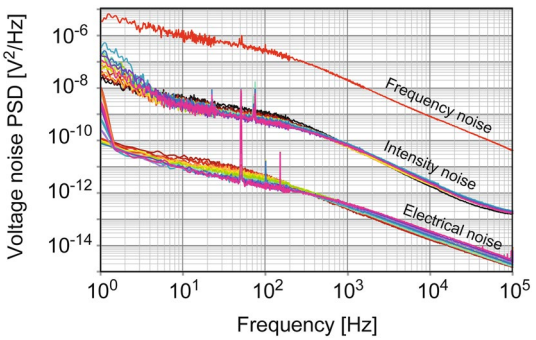

Fig. 8 Comparison of the electrical noise (voltage across the laser) and optical noise (both intensity and frequency noise) measured in QCL #sbcw-4821. Electrical noise spectra were measured at $T = 6$ °C and various currents. Laser intensity noise was measured out of a N_2O absorption line at $T = 10$ °C and various currents. Frequency noise was recorded on the side of a N_2O transition at $T = 6$ °C and $I = 590$ mA; the raw spectra of the photodiode voltage are shown here without conversion into frequency noise using the discriminator slope

lasers of the type #sbcw-48xx or in laser #sbcw-5502). The device #sbcw-5503 even shows a voltage noise that tends to slightly decrease at higher current.

Figure 10 displays another representation of the complete set of data obtained at 25 °C for the different lasers. Here, the results are grouped as a function of the six different QCLs processes previously listed in Table 1. This representation shows an influence of the process on the noise level: Lasers produced from the same process roughly tend to have a similar noise level, even if the data show a large spread over the different considered operation cur-rents. In addition, a significant variability among the lasers from the same process also results from the differ-ent considered parameters, such as the laser length, width, as listed in Table 2. The lower noise generally achieved in ridge-waveguide lasers is clearly seen in the representation of Fig. 10.

4.2 Data processing for statistical analysis

In order to implement some statistical analysis to assess the importance of the selected parameters in the noise generation, it was necessary to build a consistent set of observables encompassing the selected parameters and their respective modalities. Ideally, two different modalities for each parameter should be considered, leading to a set of 32 observables to completely cover the 5-parameter space previously defined. For each of these observables, a measurable quantity that is a representative of the corresponding QCL noise also needs to be defined. From the large set of data encompassed in the measured noise spectra, the integrated value of the voltage noise obtained over the whole spectrum (1 Hz–100 kHz) was computed and used as the response parameters to the selected independent input parameters. We label Z this integrated voltage noise.

Due to the considered QCLs procurement methodology consisting of a selection of existing lasers, it was not possible to have only two different values for each parameter. The available devices thus contained some intrinsic variability that added an intrinsic uncertainty on the response parameter Z, in addition to the experimental uncertainty on the measured electrical noise. Therefore, we defined for each parameter a threshold value delimiting two modalities (high vs. low) that are listed in Table 3. The two modalities (low/high) for the laser current were defined with respect to the threshold I_{th} and the rollover current I_{roll} by introducing the normalized current $I_n = (I - I_{th}) / (I_{roll} - I_{th})$.

BH devices present in general lower optical losses and a higher thermal conductance than ridge-waveguide lasers. Therefore, they are generally more suitable for commercial

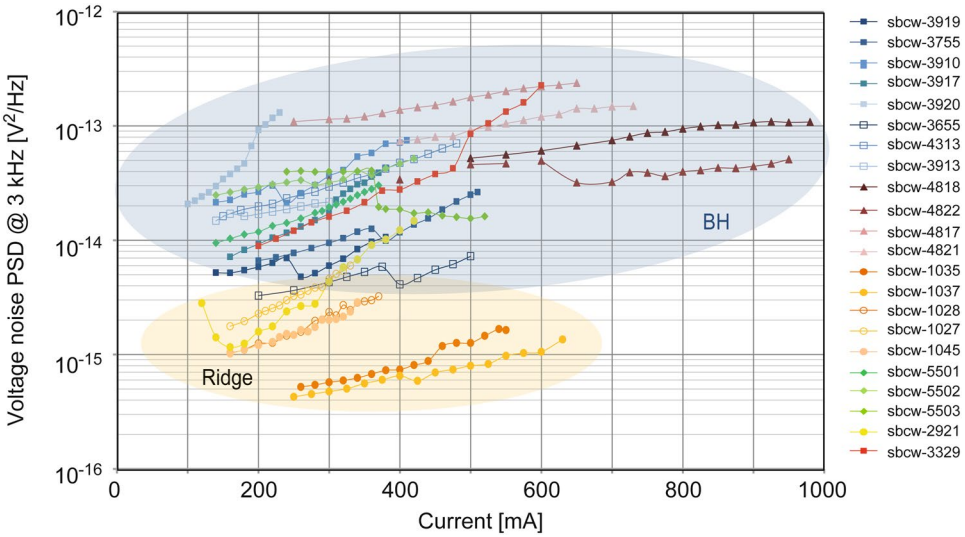

Fig. 9 Dependence of the 3-kHz frequency component of the voltage noise PSD in all investigated QCLs as a function of the operating current. All measurements were realized at a laser temperature of 25 °C. The *orange* and *blue* areas enclose the ridge and BH lasers, respectively

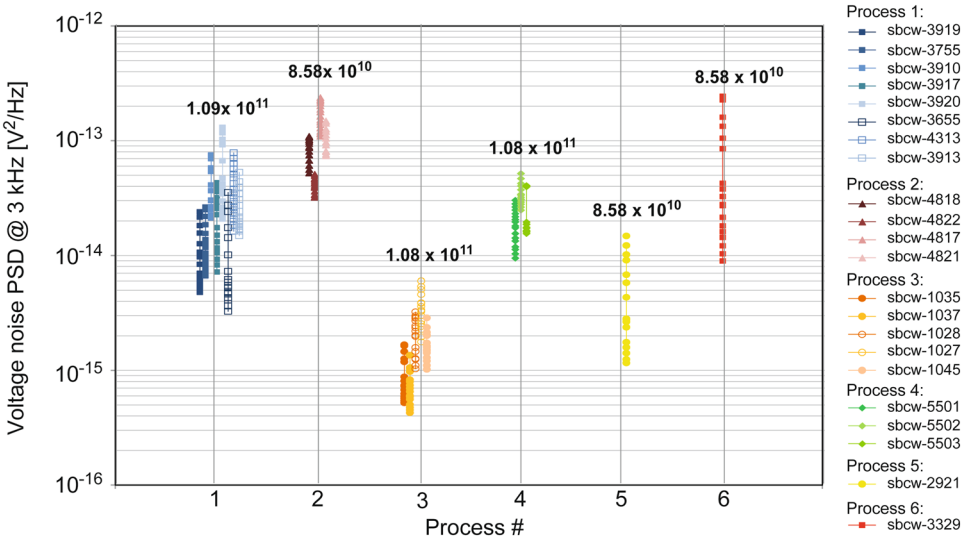

Fig. 10 Overall representation of the voltage noise measured in the different investigated QCLs classified in six different types of process. The doping level n for each process (in cm^{-2}) is indicated in the graph. The 3-kHz frequency component of the voltage noise is shown here for each laser at various operating currents (each point corresponds to a different current ranging from sub-threshold to rollover). Lasers from the same process generally have different parameters (such as length or width), which contributes to the observed noise variability. All measurements were realized at a laser temperature of 25 °C

Table 3 List of selected independent parameters with their defined modalities

Independent parameters	Modalities	
	High	Low
Laser length (mm)	L ≥ 2.25 (long)	S ≤ 1.5 (short)
Laser width (μm)	W ≥ 13.5 (wide)	N ≤ 12.5 (narrow)
Heat sink temperature (°C)	HT > 15 (high)	LT ≤ 15 (low)
Laser current level (%)	HI > 0.6 (high)	LI < 0.4 (low)

purpose. Due to the small number of ridge lasers available in this study, a complete set of observables including this type of lasers could not be built. Therefore, a full factorial experimental plan composed of 32 observables associated with the four independent parameters listed in Table 3, each considered with one repetition, was built using only BH devices. In addition, another reduced set of observables was specifically made to include both BH and ridge lasers. The used parameters in this case were the laser process geometry (RWG, BH), the waveguide width (W, N), the temperature (HT, LT), and the current (LI, HI). The length was set in this case to short (S). For these two sets of observables, it was necessary in some cases to build a repetition with the same device, but with a different noise measurement in order to achieve a complete set of observables with one repetition.

4.3 Analysis of variance

An ANOVA was realized using the *R* software [30] in order to analyze the measured noise data and to assess the significance of the considered parameters in the observed noise variability. The results of the ANOVA performed

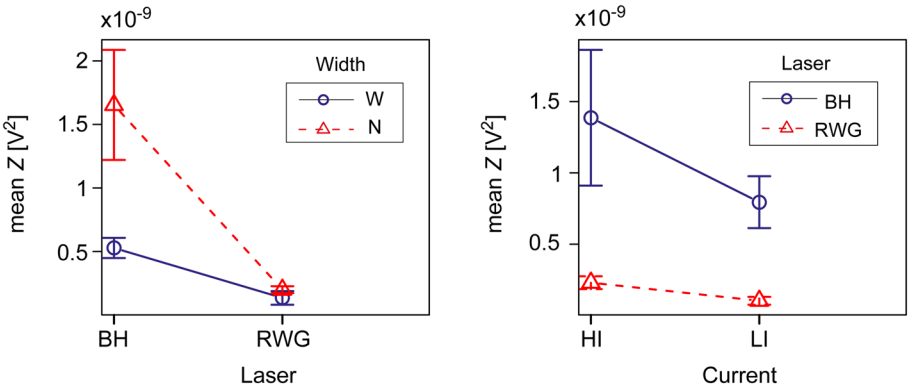

Fig. 11 Plots of the mean of the integrated voltage noise Z as a function of the laser type (*BH* vs. *RWG*), width (*W* vs. *N*), and current (*HI* vs. *LI*) modalities defined in Table 3

on the first data set made of BH lasers only showed that the laser width was the statistically most significant parameter impacting the observed noise variance. Then, some interactions between two parameters also had some influence on the noise level, but the observed noise variability was only partially explained by these parameters. Basically, short and wide BH devices operated close to threshold are statistically expected to have a lower electrical noise, independently of the operating temperature within the considered range. One must emphasize here that this statement concerns the electrical noise of the lasers. This is not in contradiction with previous observation stating that for a similar electrical noise, a long device tends to have a lower optical frequency noise [28] resulting from its smaller thermal resistance that contributes to the electrical-to-frequency noise conversion according to Eq. (3).

The ANOVA performed on the restricted data set encompassing both BH and ridge QCLs showed that the most significant parameters were the type of laser and the width of the waveguide. Figure 11 shows a graphical representation of these results, in the form of plots of the mean value of the integrated electrical noise Z as a function of the *Type:Width* and the *Current:Type* parameters. The observed level of noise for the ridge lasers is significantly lower than for the BH devices, which is in agreement with previous qualitative results displayed in Figs. 9 and 10, as well as from former observations for 4.6-μm QCLs at low temperature [28]. However, one should mention that all BH lasers used in this study were fabricated by MOVPE, while ridge lasers were produced by MBE. Therefore, one cannot completely exclude an impact of the growth process on the observed noise. However, this is quite unlikely and a simi-lar voltage noise has been reported in Ref. [13] for ridge lasers grown by MOVPE as observed in our case for MBE-grown ridge QCLs.

In addition, the width of the device has a prominent effect in BH-QCLs, narrow waveguide devices having a higher noise than broader devices.

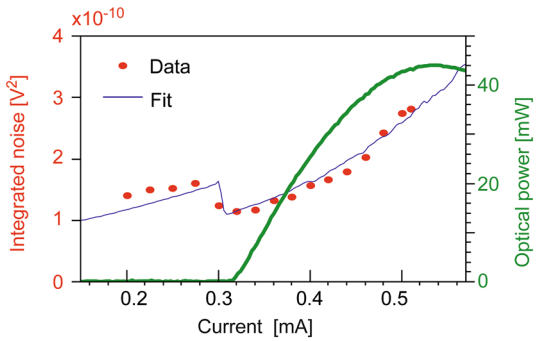

Fig. 12 **a** Integrated electrical noise (*red circles*) and output power (*thick green line*) as a function of the drive current displayed for laser sbcw-3755. The *thin blue* lines represent a fit of the experimental data by the function defined by Eq. (4). The R^2 value is 0.98

4.4 A potential additional noise source in BH-QCLs

The possibility to perform electrical noise measurements not only under laser emission, but also below threshold in the absence of lasing, allowed observing a reduction in the electrical noise at the laser threshold in some devices. A similar "kink" occurring in the laser current–voltage (I–V) curve suggested a possible link between the observed noise and the laser differential resistance. An empirical model of the magnitude of the integrated noise Z as a function of the differential resistance dV/dI (Eq. 4) has been tested on the experimental noise data:

$$Z = A\left(\frac{dV}{dI}\right)^2 I^2 + B. \tag{4}$$

The model proved to fit the data very well for some BH lasers as shown for a particular device in Fig. 12, but not for all. In total, this fit procedure was tested over more than 40 different data sets obtained from 20 devices essentially measured at the two laser temperatures of 5 and 25 °C. A fraction of 41 % of these fits, containing both BH and ridge lasers, showed anR^2 value higher than 0.9, which proves

that the behavior shown in Fig. 12 does not represent an isolated case. The analysis using this simple model suggests a link between the laser differential resistance and the noise. This is a property of Hooge's model of 1/*f* noise that attributes the origin of flicker noise to a fluctuation of the carrier number [23]. We will propose below another possible interpretation for the higher noise observed in BH-QCLs.

The statistical analysis done in the previous Sect. 4.3 allowed us to gain some insight on the influence of the analyzed parameters on the noise. However, it is clear that the noise in BH devices cannot be fully explained by the analyzed parameters. While a larger laser width tends to reduce the noise in BH lasers, the observed difference between BH and ridge devices strongly suggests that a fundamental difference causes an excess of noise in BH-QCLs. The main difference between the two considered types of lasers consists in the presence of a lateral insulator in BH lasers (see Fig. 1). Additional current leakages or spare injection channels occurring at the interface between the active region and the insulator could contribute to the observed excess noise in BH lasers. Such an assumption is also consistent with the observation that broader BHs lead to a lower noise, as the relative importance of the lateral surfaces is reduced.

The noise behavior observed in BH-QCLs at room temperature in this study and as a function of temperature in our former work [12] shows similar features as reported by Güttler et al. [31] for Schottky diodes. At low temperature, they showed that the electrical noise of the diodes increased upon cooling, while at room temperature an increase in the noise with the injected current was observed. Explaining their observations, Güttler et al. [31] have shown a cor-relation between the magnitude of the observed noise and the strength of spatial inhomogeneities at the metal–semi-conductor interface in Schottky diodes. An analogy can be made between the described structure and the BH laser configuration, where not only a highly doped cladding act-ing somehow like a metal is deposited onto an insulator, but periodically doped layers are also in contact with the lat-eral insulator. These interfaces may thus behave in a similar way as Schottky diodes, which suggest that Schottky-type contacts in BH lasers could be a potential additional noise source.

Schottky noise may also be a contribution in ridge QCLs, but limited to the laser contacts. The additional lateral contribution that has a significant impact on BH-QCLs is not present in ridge lasers.

5 Discussion and conclusion

1/*f* noise in near-infrared semiconductor laser diodes has been the subject of numerous studies in the past, with somehow contradictory outcomes. Whereas several studies reported a strong correlation between optical noise (either frequency or intensity noise) and terminal voltage noise [32–36] as we observed here for mid-infrared QCLs, some others, on the contrary, assessed the absence of any cor-relation between these two quantities [37]. The origin of 1/*f* noise in near-infrared semiconductor light sources has also been largely discussed in various devices including laser diodes at 0.8 [37], 1.3 [38] and 1.55 μm [32, 35], but also in superluminescent diodes [39]. Different poten-tial explanations have been suggested about the origin of flicker noise, such as the appearance of some sort of cur-rent fluctuations due to the presence of carrier traps in the vicinity of the active region, perhaps related to strains resulting from lattice mismatch close to the heterojunc-tion interfaces [37], or induced by different types of non-radiative carrier recombination such as surface and inter-face recombination or recombination at deep levels [35]. Leakage currents were also reported as a contributor to frequency noise in semiconductor laser diodes; experimen-tal results show that frequency noise increased in lasers with larger leakage currents [34]. The presence of leakage currents in laser diodes was assessed from particular fea-tures observed in the shape of their current–voltage char-acteristic, in particular deviations from an ideal diode I–V response [34, 38].

All QCLs investigated in this study were operating at a similar voltage of 7–10 V. However, their threshold current was extending over a quite broad range, and the lasers were thus operated at significantly different currents. One noticed as a general trend in this study that lasers displaying the highest voltage noise also exhibited larger deviations of their current–voltage characteristic from an ideal response, e.g., operation at a higher bias current. This observation supports the contribution of leakage currents, resulting in nonradiative recombination, to the laser voltage noise.

In the experimental study of noise in QCLs reported here, we showed that BH lasers tend to have a higher noise than ridge-waveguide lasers. Furthermore, the noise increases when decreasing the width of BH lasers. Our interpretation is that additional current leakages or spare injection channels may occur at the interface between the active region and the lateral insulator, leading to the observed excess noise in BH lasers. Furthermore, Schottky-type contacts occurring at the interface between the n-doped regions, i.e., cladding and gain medium, and the lateral insulator could be a potential source of additional noise in some BH lasers. This was observed as a slight reduction in the integrated terminal voltage noise occurring at the laser threshold, following the dependence of the laser differential resistance $I{\cdot}dV/dI$. Such behavior has been observed in several BH-QCLs in this study.

A link between the level of frequency noise and the behavior of the laser differential resistance was previously reported in semiconductor laser diodes and was explained in terms of leakage currents [38]. Based on this observation, low-frequency 1/*f* noise has been proposed as a sensitive measure of the quality and reliability of near-infrared laser diodes [32, 36], by indicating the presence of intrinsic defects or fabrication imperfections that can act as deep traps or recombination centers in the semiconductor structure. In the QCLs investigation reported here, we did not see any evidence of a direct relation between noise and laser reliability. Higher output powers and laser operation temperatures are made possible by the use of BH geometry in comparison with ridge-waveguide configurations, owing to its better thermal dissipation capabilities. However, ridge QCLs showed a significantly lower electrical noise. In addition, one of the devices of our study suddenly suffered from some accidental degradation and its threshold current increased so that the device was no longer lasing at room temperature. Despite this serious degradation, the electri-cal noise of this QCL did not show any significant change compared to the noise measured before the degradation.

To conclude, we showed that frequency noise in free-running QCLs is of electrical origin and is not directly related to the optical properties of the lasers. It is induced by fluctuations arising in the electrons flow through the device and is affected in particular by leakage currents. In this sense, we showed that a broad BH geometry leads to a lower noise than a narrow structure as the impact of the lateral surfaces is reduced. In contrast, ridge-waveguide lasers do not suffer from this additional noise which might explain the lower noise observed in these lasers. The origin of this noise has been recently described by fluctuating charge-dipoles by Yamanishi et al. [13].

Acknowledgments This work was financed by the Swiss Space Office (SSO) in the frame of the MdP (Positioning measures) program. The authors from University of Neuchatel are also grateful to the Swiss National Science Foundation for additional financial support.

References

1. J. Faist, F. Capasso, D.L. Sivco, C. Sirtori, A.L. Hutchinson, A.Y. Cho, Quantum cascade lasers. Science **264**, 553–556 (1994)
2. A. Gambetta, D. Gatti, A. Castrillo, N. Coluccelli, G. Galzerano, P. Laporta, L. Gianfrani, M. Marangoni, Comb-assisted spectroscopy of CO_2 absorption profiles in the near- and mid-infrared regions. Appl. Phys. B **109**(3), 385–390 (2012)
3. S. Borri, I. Galli, F. Cappelli, A. Bismuto, S. Bartalini, P. Cancio, G. Giusfredi, D. Mazzotti, J. Faistd, P. De Natale, Direct link of a mid-infrared QCL to a frequency comb by optical injection. Opt. Lett. **37**, 1011–1013 (2012)
4. A.A. Mills, D. Gatti, J. Jiang, C. Mohr, W. Mefford, L. Gianfrani, M. Fermann, I. Hartl, M. Marangoni, Coherent phase lock of a 9 μm quantum cascade laser to a 2 μm thulium optical frequency comb. Opt. Lett. **37**, 4083–4085 (2012)
5. A. Gambetta, D. Gatti, A. Castrillo, G. Galzerano, P. Laporta, L. Gianfrani, M. Marangoni, Mid-infrared quantitative spectroscopy by comb-referencing of a quantum-cascade-laser: application to the CO_2 spectrum at 4.3 μm. Appl. Phys. Lett. **99**(25), 251107 (2011)
6. P.L.T. Sow, S. Mejri, S.K. Tokunaga, O. Lopez, A. Goncharov, B. Argence, C. Chardonnet, A. Amy-Klein, C. Daussy, B. Darqui, A widely tunable 10 μm quantum cascade laser phase-locked to a state-of-the-art mid-infrared reference for precision molecular spectroscopy. Appl. Phys. Lett. **104**, 264101 (2014)
7. S. Bartalini, S. Borri, P. Cancio, A. Castrillo, I. Galli, G. Giusfredi, D. Mazzotti, L. Gianfrani, P. De Natale, Observing the intrinsic linewidth of a quantum-cascade laser: beyond the Schawlow–Townes limit. Phys. Rev. Lett. **104**, 083904 (2010)
8. T. Aellen, R. Maulini, R. Terazzi, N. Hoyler, M. Giovaninni, S. Blaser, L. Hvozdara, J. Faist, Direct measurement of the linewidth enhancement factor by optical heterodyning of an amplitude-modulated quantum cascade laser. Appl. Phys. Lett. **89**, 091121 (2006)
9. T.L. Myers, R.M. Williams, M.S. Taubman, C. Gmachl, F. Capasso, D.L. Sivco, J.N. Baillargeon, A.Y. Cho, Free-running frequency stability of mid-infrared quantum cascade lasers. Opt. Lett. **27**(3), 170–172 (2002)
10. L. Tombez, J. Di Francesco, S. Schilt, G. Di Domenico, J. Faist, P. Thomann, D. Hofstetter, Frequency noise of free-running 4.6 μm DFB quantum cascade lasers near room temperature. Opt. Lett. **36**(16), 3109–3111 (2011)
11. S. Bartalini, S. Borri, I. Galli, G. Giusfredi, D. Mazzotti, T. Edamura, N. Akikusa, M. Yamanishi, P. De Natale, Measuring frequency noise and intrinsic linewidth of a room-temperature DFB quantum cascade laser. Opt. Express **19**(19), 17996–18003 (2011)
12. L. Tombez, S. Schilt, J. Di Francesco, P. Thomann, D. Hofstetter, Temperature dependence of the frequency noise in a mid-IR DFB quantum cascade laser from cryogenic to room temperature. Opt. Express **20**(7), 6851–6859 (2012)
13. M. Yamanishi, T. Hirohata, S. Hayashi, K. Fujita, K. Tanaka, Electrical flicker-noise generated by filling and emptying of impurity states in injectors of quantum cascade lasers. J. Appl. Phys. **116**, 183106 (2014)
14. S. Borri, S. Bartalini, P.C. Pastor, I. Galli, G. Giusfredi, D. Mazzotti, M. Yamanishi, P. De Natale, Frequency-noise dynamics of mid-infrared quantum cascade lasers. IEEE J. Quantum Electron **47**, 984–988 (2011)
15. L. Tombez, S. Schilt, D. Hofstetter, T. Südmeyer, Active linewidth-narrowing of a mid-IR quantum cascade laser without optical reference. Opt. Lett. **38**(23), 5079–5082 (2013)
16. K. Knabe, P.A. Williams, F.R. Giorgetta, C.M. Armacost, S. Crivello, M.B. Radunsky, N.R. Newbury, Frequency characterization of a swept- and fixed-wavelength external-cavity quantum cascade laser by use of a frequency comb. Opt. Express **20**, 12432–12442 (2012)
17. R.M. Williams, J.F. Kelly, J.S. Hartman, S.W. Sharpe, M.S. Taubman, J.L. Hall, F. Capasso, C. Gmachl, D.L. Sivco, J.N. Baillargeon, A.Y. Cho, Kilohertz linewidth from frequency-stabilized mid-infrared quantum cascade lasers. Opt. Lett. **24**, 1844–1846 (1999)
18. F. Cappelli, I. Galli, S. Borri, G. Giusfredi, P. Cancio, D. Mazzotti, A. Montori, N. Akikusa, M. Yamanishi, S. Bartalini, P. De Natale, Subkilohertz linewidth room-temperature mid-infrared quantum cascade laser using a molecular sub-Doppler reference. Opt. Lett. **37**, 4811–4813 (2012)
19. M.S. Taubman, T.L. Myers, B.D. Cannon, R.M. Williams, F. Capasso, C. Gmachl, D.L. Sivco, A.Y. Cho, Frequency

stabilization of quantum-cascade lasers by use of optical cavities. Opt. Lett. **27**, 2164–2166 (2002)
20. E. Fasci, N. Coluccelli, M. Cassinerio, A. Gambetta, L. Hilico, L. Gianfrani, P. Laporta, A. Castrillo, G. Galzerano, Narrow-linewidth quantum cascade laser at 8.6 μm. Opt. Lett. **39**(16), 4946–4949 (2014)
21. I. Sargachev, R. Maulini, A. Bismuto, S. Blaser, T. Gresch, Y. Bidaux, A. Müller, S. Schilt, T. Südmeyer, All-electrical frequency noise reduction and linewidth narrowing in quantum cascade lasers. Opt. Lett. **39**(22), 6411–6414 (2014)
22. A.L. McWorther, "1/*f* noise and germanium surface properties", in *Semiconductor Surface Physics*, ed. by R.H. Kingston (University of Pennsylvania, Philadelphia, 1957), pp. 207–228
23. F.N. Hooge, 1/*f* noise is no surface effect. Phys. Lett. A **29**, 139–140 (1969)
24. J. Faist, D. Hofstetter, M. Beck, T. Aellen, M. Rochat, S. Blaser, Bound-to-continuum and two-phonon resonance, quantum-cascade lasers for high duty cycle, high-temperature operation. Quantum Electron Lett. **38**, 533–546 (2002)
25. L. Tombez, S. Schilt, J. Di Francesco, T. Führer, B. Rein, T. Walther, G. Di Domenico, D. Hofstetter, P. Thomann, Linewidth of a quantum cascade laser assessed from its frequency noise spectrum and impact of the current driver. Appl. Phys. B **109**(3), 407–414 (2012)
26. E. Rubiola, F. Vernotte, The cross-spectrum experimental method http://arxiv.org/abs/1003.0113
27. T. Aellen, S. Blaser, M. Beck, D. Hofstetter, J. Faist, E. Gini, Continuous-wave distributed-feedback quantum-cascade lasers on a Peltier cooler. Appl. Phys. Lett. **83**, 1929 (2003)
28. L. Tombez, S. Schilt, G. Di Domenico, S. Blaser, A. Muller, T. Gresch, B. Hinkov, M. Beck, J. Faist, D. Hofstetter, Physical Origin of Frequency Noise and Linewidth in Mid-IR DFB Quantum Cascade Lasers. CLEO. San Jose, USA; June 9–14, 2013, oral #CM1 K.3
29. L. Tombez, F. Cappelli, S. Schilt, G. Di Domenico, S. Bartalini, D. Hofstetter, Wavelength tuning and thermal dynamics of continuous-wave mid-IR distributed feedback quantum cascade laser. Appl. Phys. Lett. **103**(3), 031111–031115 (2013)
30. http://www.r-project.org/
31. H.H. Güttler, J.H. Werner, Influence of barrier inhomogeneities on noise at Schottky contacts. Appl. Phys. Lett. **56**, 1113 (1990)
32. G. Letal, S. Smetona, R. Mallard, J. Matukas, V. Palenskis, S. Pralgauskaite, Reliability and low-frequency noise measurements of InGaAsP multiple quantum well buried-heterostructure lasers. J. Vac. Sci. Technol. A **20**(3), 1061–1066 (2002)
33. W.H. Richardon, Y. Yamamoto, Quantum correlation between the junction-voltage fluctuation and the photon-number fluctuation in a semiconductor laser. Phys. Rev. Lett. **66**(15), 1963–1966 (1991)
34. R.E. Bartolo, C.K. Kirkendall, V. Kupershmidt, S. Siala, Achieving narrow linewidth, low phase noise external cavity semiconductor lasers through the reduction of 1/f noise, *Proceedings SPIE* 6133, Novel In-Plane Semiconductor Lasers V, 61330I (22 Feb 2006)
35. R. Hakimi, M.-C. Amman, Reduction of 1/f carrier noise in InGaAsP-InP heterostructures by sulphur passivation of facets. Semicond. Sci. Technol. **12**, 778–780 (1997)
36. Y. Dai, J. Shi, X. Zhang, J. Shi, E. Jin, A study of optical noise measurements as a reliability estimation for laser diodes. Microelectron. Reliab. **35**(4), 731–734 (1995)
37. A. Dandridge, H.F. Taylor, Correlation of low-frequency intensity and frequency fluctuations in GaAlAs lasers. IEEE J. Quantum Electron. **18**(10), 1738–1750 (1982)
38. I.A. Garmash. V.N. Morozov, A.T. Semenov, M.A. Sumarokov, V.R. Shidlovskii, Leakage currents and 1/f noise in buried InGaAsP-InP heterostructure lasers. J. Quantum Electron. **20** (8), (1990)
39. A. Dandridge, H.F. Taylor, Noise and correlation effects in GaAlAs broad-band sources. J. Lightwave Technol. **5**(5), 689–693 (1987)